arXiv:cond-mat/0205325v1 [cond-mat.mtrl-sci] 15 May 2002

Surface anchoring on liquid crystalline polymer brushes

Harald Lange[†,‡] and Friederike Schmid[†,*]

† *Fakultät für Physik, Universität Bielefeld, 33615 Bielefeld, Germany*

∗ *Telephone: ++49-521-1066191, E-mail:* schmid@physik.uni-bielefeld.de

‡ *Institut für Physik, Universität Mainz, 55099 Mainz, Germany*

Abstract

We present a Monte Carlo study of the surface anchoring of a nematic fluid on swollen layers of grafted liquid crystalline chain molecules. The liquid crystalline particles are modeled by soft repulsive ellipsoids, and the chains are made of the same particles. An appropriately modified version of the configurational bias Monte Carlo algorithm is introduced, which removes and redistributes chain bonds rather than whole monomers. With this algorithm, a wide range of grafting densities could be studied.

The substrate is chosen such that it favors a planar orientation (parallel to the surface). Depending on the grafting density, we find three anchoring regimes: planar, tilted, and perpendicular alignment. At low grafting densities, the alignment is mainly driven by the substrate. At high grafting densities, the substrate gradually loses its influence and the alignment is determined by the structure of the interface between the brush and the pure solvent instead.

Key words: liquid crystals, surface anchoring
PACS: 61.30.Hn, 61.30.Vx

1. Introduction

Liquid crystals have fascinated condensed matter physicists, chemists and material scientists for many decades [1,2] – first, because they exhibit a large number of beautiful phases with intriguing symmetries and interesting material properties, and second, because of their technological use, particularly in the domain of display devices. One important aspect for technical applications is the so-called surface anchoring [3–5]: Surfaces orient nearby molecules, and these in turn orient the whole bulk of the liquid crystal. Alignment layers are key components of liquid crystal display devices [5]. In particular, one is interested in designing surfaces which orient liquid crystals in a well-defined way in any desired direction.

Possible candidates are liquid crystalline polymer brushes [6–10]. Halperin and Williams [6] have suggested to create a situation where a substrate which favors planar anchoring (parallel to the surface) competes with a stretched main-chain liquid-crystalline brush which favors homeotropic anchoring (perpendicular to the surface). They predicted that this conflict would result in tilted anchoring above a critical grafting density Σ_c. In their scenario, the transition between planar and tilted anchoring is continuous. Above the transition, the grafting density can be used to tune the anchoring

angle.

Experimentally, dense liquid crystalline polymer brushes have been prepared [9], and their alignment properties have been studied [10]. So far, the conditions in the experiments were such that the substrate and the brush favor the same type of alignment. However, a competition as required by the scenario of Halperin and Williams can be introduced by a straightforward modification of the substrate [10].

Motivated by that work, we have investigated the consequences of such a competition by Monte Carlo simulations of an idealized liquid crystal model. We have studied brushes of liquid crystalline polymers in a nematic solvent on a substrate which favors planar anchoring. The relaxation times in such systems are very high. Therefore, we have implemented a new version of the configurational bias Monte Carlo algorithm [11–14]: Chains are broken up such that their monomers turn into solvent particles, and solvent particles are linked together to form new chains. With this algorithm, a wide range of grafting densities could be considered. We shall see that the resulting anchoring scenario turns out to be quite rich.

We introduce the simulation model in the next section, and describe the algorithm in the third section. The results are presented and discussed in section 4. We summarize and conclude in the last section.

2. The Simulation Model

Our system consists of soft ellipsoidal particles with elongation $\kappa = \sigma_{\text{end-end}}/\sigma_{\text{side-side}} = 3$. Two particles i and j with orientations $\mathbf{u}_i$ and $\mathbf{u}_j$ separated by the center-center vector $\mathbf{r}_{ij}$ interact via the purely repulsive pair potential

$$V_{ij} = \begin{cases} 4\epsilon_0\,(X_{ij}^{12} - X_{ij}^{6}) + \epsilon_0 \;:\; X_{ij}^{6} > 1/2 \\ 0 \qquad\qquad\qquad\qquad\quad :\; \text{otherwise} \end{cases} . \tag{1}$$

where $X_{ij} = \sigma_0/(r_{ij} - \sigma_{ij} + \sigma_0)$ and

$$\sigma_{ij} = \sigma_0 \left\{ 1 - \frac{\chi}{2}\Big[\frac{(\mathbf{u}_i\cdot\hat{\mathbf{r}}_{ij} + \mathbf{u}_j\cdot\hat{\mathbf{r}}_{ij})^2}{1+\chi\mathbf{u}_i\cdot\mathbf{u}_j} + \frac{(\mathbf{u}_i\cdot\hat{\mathbf{r}}_{ij} - \mathbf{u}_j\cdot\hat{\mathbf{r}}_{ij})^2}{1-\chi\mathbf{u}_i\cdot\mathbf{u}_j}\Big] \right\}^{-1/2} \tag{2}$$

with $\chi = (\kappa^2-1)/(\kappa^2+1)$. The function σ_{ij} approximates the contact distance between the two ellipsoids in the direction $\hat{\mathbf{r}}_{ij} = \mathbf{r}_{ij}/r_{ij}$ [15].

Solvent and chain particles have the same non-bonded interactions. In addition, chain monomers are connected by anharmonic springs of length b with equilibrium length b_0 and a logarithmic cut-off at $|b - b_0| = b_s$. At $|b - b_0| < b_s$, the spring potential is given by

$$V_s(b) = -k_s/2\, b_s^2 \ln[1 - (b-b_0)^2/b_s^2)\,]. \tag{3}$$

The direction of a bond is given by the unit vector $\hat{\mathbf{b}}$. A stiffness potential

$$V_a(\mathbf{u}, \hat{\mathbf{b}}_1, \hat{\mathbf{b}}_2) = -k_a\,(|\mathbf{u}\hat{\mathbf{b}}_1| + |\mathbf{u}\hat{\mathbf{b}}_2| + 2\,\hat{\mathbf{b}}_1\hat{\mathbf{b}}_2) \tag{4}$$

is imposed, which penalizes non-zero angles between the orientation $\mathbf{u}$ of a monomer and its two adjacent bonds $\hat{\mathbf{b}}_1$ and $\hat{\mathbf{b}}_2$. The system is confined by hard walls at two sides $z = 0$ and $z = L_z$: The distance between the walls and the centers of ellipsoids, which have an angle θ with respect to the surface normal, must exceed

$$d_z(\theta) = \sigma_0/2\,\sqrt{1 + \cos^2(\theta)\,(\kappa^2 - 1)}. \tag{5}$$

The chains are grafted to the walls at one end, the grafting points are arranged on a regular square lattice.

We have studied systems with roughly $N = 2000$ solvent particles (the numbers varied in the different runs) and up to 242 chains of four monomers. The simulation boxes were rectangular of size $L_\parallel \times L_\parallel \times L_z$ with periodic boundary conditions in the lateral directions and fixed boundary conditions in the z direction. The thickness L_z was allowed to fluctuate, so that the simulations could be performed at constant pressure. The lateral size $L_\parallel = 12\sigma_0$ was kept fixed in order to maintain a constant grafting density Σ. Trial moves included monomer displacements, monomer rotations, rescaling of L_z, and the configurational bias moves described in the next section. The initial configuration was set up such that all particles pointed in the x direction. The system was then equilibrated over at least 1 million Monte Carlo steps, and data were collected over 5 or more million Monte Carlo steps.

One "Monte Carlo step" includes on average N attempts of monomer displacements, $2N$ attempts of monomer rotations, one attempt of L_z rescaling, and one attempt of a configurational bias move.

The model parameters chosen were $k_s = k_a = 10.$, $b_0 = 4.$ and $b_s = 0.8$. Here and throughout, we use scaled units defined in terms of ϵ_0, σ_0, and the Boltzmann constant k_B. Unless stated otherwise, the simulations were performed at constant temperature $T = 0.5$ and constant pressure $P = 3$. The average number density in the bulk was $\langle\rho\rangle = 0.313$.

3. Configurational Bias Monte Carlo in a Solvent

The most frequently used continuous space version of the configurational bias Monte Carlo algorithm [12,16] removes chains from the system and inserts new monomers into the system. However, this method is not effective in our system, because the space is densely filled with monomer and solvent particles, and little free volume for new particles is available. Therefore, we have resorted to a different scheme. Instead of removing the monomers of a chain, we only remove the connecting bonds and redistribute them such that new chains are formed from solvent particles. This method resembles closely the lattice version of the configurational bias Monte Carlo algorithm [12]. The only difference is that the lattice is now random, with "lattice sites" given by the centers of solvent or monomer particles.

In practice, we proceed as follows: First, we remove all the bonds from a randomly chosen chain. Then we find all n_1 solvent particles, which are at a distance $b \in [b_0 - b_s, b_0 + b_s]$ from the grafting point, and choose one of them according to the Boltzmann probability

$$P_1 = \frac{1}{Z_1} \exp\Big[- \frac{V_s(b_1) + k_a(1 - |\mathbf{u}_1 \hat{\mathbf{b}}_1|)}{T} \Big] \qquad (6)$$

Here b_1 is the length of the bond between the grafting point and the particle, $\hat{\mathbf{b}}_1$ its direction, and $\mathbf{u}_1$ the orientation of the particle. The normalization factor Z_1 is the sum

$$Z_1 = \sum_{j=1}^{n_1} \exp\Big[- \frac{V_s(b_{1;j}) - k_a|\mathbf{u}_{1;j}\hat{\mathbf{b}}_{1;j}|}{T} \Big] \qquad (7)$$

over the Boltzmann factors for all n_1 potential candidates j. We continue in the same spirit and construct a new trial chain monomer by monomer: Given the $(\alpha - 1)$th monomer, we identify all n_α solvent particles at the distance $b \in [b_0 - b_s, b_0 + b_s]$ from the $(\alpha - 1)$th monomer, and pick one with the probability

$$P_\alpha = \frac{1}{Z_\alpha} \exp\Big\{ - \frac{1}{T} \big[V_s(b_\alpha) - k_a(|\mathbf{u}_{\alpha-1}\hat{\mathbf{b}}_\alpha| + 2\hat{\mathbf{b}}_{\alpha-1}\hat{\mathbf{b}}_\alpha + |\mathbf{u}_\alpha\hat{\mathbf{b}}_\alpha|)\big] \Big\} \qquad (8)$$

with

$$Z_\alpha = \sum_{j=1}^{n_\alpha} \exp\Big\{ - \frac{1}{T} \big[V_s(b_{\alpha;j}) - k_a(|\mathbf{u}_{\alpha-1}\hat{\mathbf{b}}_{\alpha;j}| + \hat{\mathbf{b}}_{\alpha-1}\hat{\mathbf{b}}_{\alpha;j} + |\mathbf{u}_{\alpha;j}\hat{\mathbf{b}}_{\alpha;j}|)\big] \Big\} \qquad (9)$$

The total probability of constructing a given new chain with M monomers is

$$P_{\text{new}} = \prod_{\alpha=1}^{M} P_\alpha. \qquad (10)$$

For the final Metropolis step, one also has to compute the probability P_{old} that the original, initially removed chain is constructed. The way to do this is exactly analogous, except that the monomers are not picked randomly. The new chain is accepted with the probability

$$W_{\text{old}\to\text{new}} = \min\big(1, \frac{P_{\text{old}}}{P_{\text{new}}} \exp(-\Delta E/T)\big), \qquad (11)$$

where ΔE is the energy difference between the old and the new chain. Since no particles were moved, ΔE only contains contributions of the bond energies. If the move is not accepted, the original chain is restored.

A similar method has been described recently by Wijmans et al [14]. The implementation of this algorithm was essential for the success of our simulations. With the new algorithm, the configurations equilibrated within a million Monte Carlo steps and reliable data for a range of grafting densities could be collected.

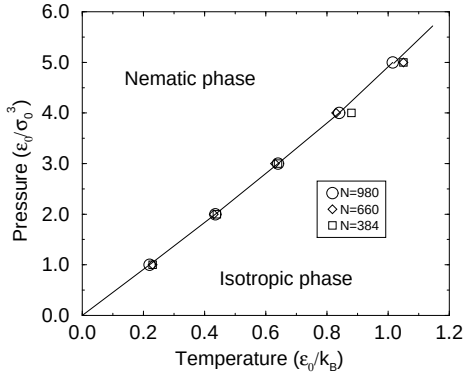

Fig. 1. Bulk phase diagram in pressure-temperature space, calculated from simulations with three different system sizes as indicated.

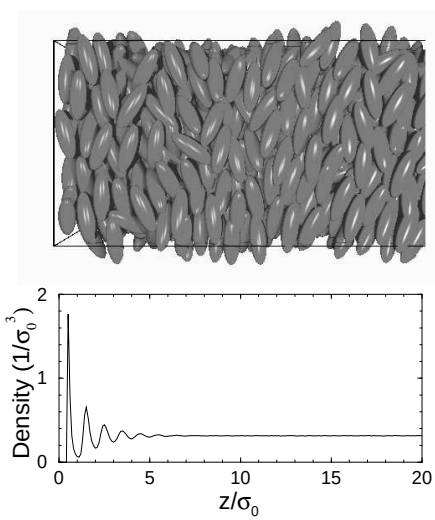

Fig. 2. Solvent in contact with the bare substrate; configuration snapshot (top) and number density profile ρ vs. z (bottom).

4. Results

Before investigating the full system, we have characterized the different constituents of our system separately.

The bulk phase diagram of the solvent particles was determined from simulations of cubic systems with periodic boundary conditions in all directions. The resulting phase diagram in $P-T$ space is shown in Figure 1. The state point of our later simulations at $T = 0.5$, $P = 3$ is well in the nematic phase. The coexistence densities at $P = 3$ are $\rho_{\text{Nematic}} \approx 0.29$, and $\rho_{\text{Isotropic}} \approx 0.28$. The systems were too small to allow for an accurate determination of the coexistence gap in $\rho - T$ space. In $P-T$ space, however, the phase boundaries are not affected much by finite size effects (Figure 1).

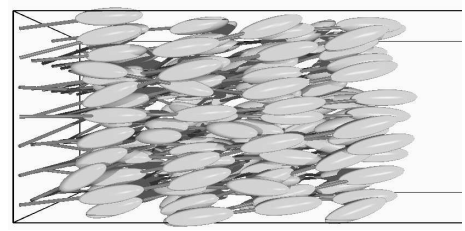

Fig. 3. Configuration snapshot of grafted chains without solvent at the grafting density $\Sigma = 0.34/\sigma_0^2$.

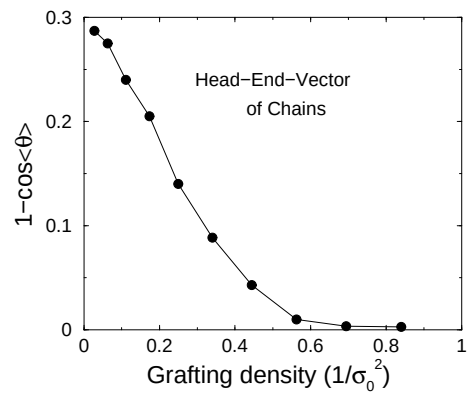

Fig. 4. Grafted chains without solvent: Average tilt angle $\langle\theta\rangle$ of the head-to-end vector of the chains as a function of the grafting density Σ.

A bare substrate without grafted chains orients the particles parallel to itself. A snapshot is shown in Figure 2. The density profile reveals strong layering effects in close vicinity to the wall, which decay rapidly in the bulk.

Finally, we have studied the behavior of brushes without solvent. A snapshot for a system with the moderate grafting density $\Sigma = 0.34/\sigma_0^2$ is shown

in Figure 3. The chains are disordered, with chain orientations distributed around $\theta = 0$ (θ being the angle with respect to the substrate normal). The average angle $\langle\theta\rangle$ of the head-to-end vectors decreases rapidly with increasing grafting density Σ (Figure 4).

We turn to the discussion of the results for the full system. Figure 5 shows a snapshot of a brush with solvent at the grafting density $\Sigma = 0.34/\sigma_0^2$. Comparing this figure with Figure 4, we note that the presence of the solvent makes the brush much more compact, i.e., the solvent particles introduce an effective attractive interaction between the chains. The chains are tilted in a common direction (Figure 5 (top)). The tilt propagates into the bulk of the system outside of the brush (Figure 5 (bottom)). As anticipated in the introduction, we thus find that a brush can induce tilt in the orientation of a nematic solvent.

The comparison of Figure 4 and Figure 6 (top) shows that the average tilt angle $\langle\theta\rangle$ of the head-to-end vector of chains increases in the presence of the solvent at all grafting densities. Most notably, the chains remained tilted up to the highest grafting densities that we considered. However, the tilt of the chains does not always produce tilted anchoring in the nematic bulk fluid. Figure 6 (bottom) demonstrates that the solvent particles have less tilt than the chain particles, and stand almost perpendicular to the surface at the highest grafting density. In fact, a closer inspection of our data shows that the remaining average angle $\langle\theta\rangle$ stems mainly from the contribution of the solvent particles inside of the brush, and from orientational disorder of the particles outside of the brush. A more detailed discussion will be presented elsewhere [17].

Figure 6 (bottom) reveals a second feature of the system: At low grafting densities, the wall aligns the solvent particles in a planar way, i. e., the alignment is basically determined by the anchoring properties of the bare substrate. At the grafting density $\Sigma \approx 0.12$, the tilt angle of solvent particles jumps discontinuously to a lower value. The data thus indicate that there is a first order transition between planar and tilted anchoring.

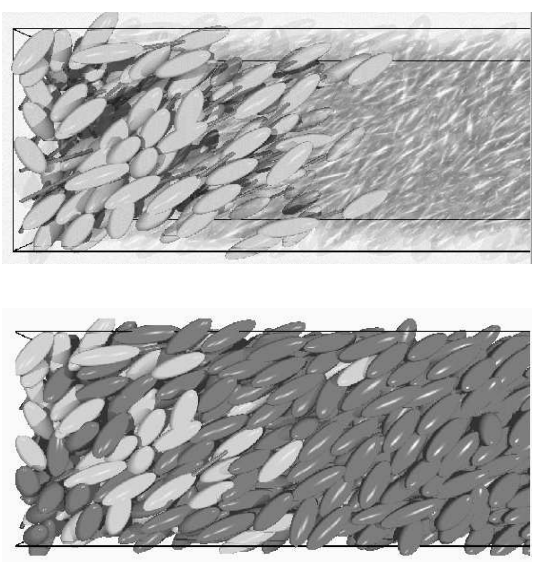

Fig. 5. Configuration snapshot of grafted chains with solvent at grafting density $\Sigma = 0.34/\sigma_0^2$. Top: Just chain monomers (solvent particles are transparent); Bottom: Chain monomers (light) and solvent particles (dark).

5. Discussion and Summary

Our simulation data disclose the following scenario: We find three different anchoring regimes. At low grafting densities, the anchoring on the wall is planar. At high grafting densities, it is homeotropic, i.e., perpendicular to the wall. Tilted anchoring can be achieved in a range of intermediate grafting densities. The transition between planar and tilted anchoring is presumably first order. The transition between tilted and perpendicular anchoring has not been studied in detail, because simulations at high grafting densities are very expensive. The data are consistent with theoretical mean field considerations [18], which suggest that it is continuous. According to theory, the anchoring behavior at high grafting densities is controlled by the structure of the interface between the polymer layer and the nematic fluid. The competition between attractive chain interac-

tions, the translational entropy of the solvent, and its elasticity, drives a continuous transition from tilted to homeotropic alignment.

From a practical point of view, low grafting densities are more interesting, because they can be realized more easily in experiments. The anchoring transition which we observe in that regime resembles that predicted by Halperin and Williams [6]. However, the underlying mechanism is probably quite different. The theory of Halperin and Williams relies on the existence of hairpins, abrupt reversals in the directions of the chains, whereas our "polymers" are much too short to support such defects. Nevertheless, the transition seems to be controlled by the organization of the chains in the polymer layer. We shall investigate this in more detail in a future publication [17].

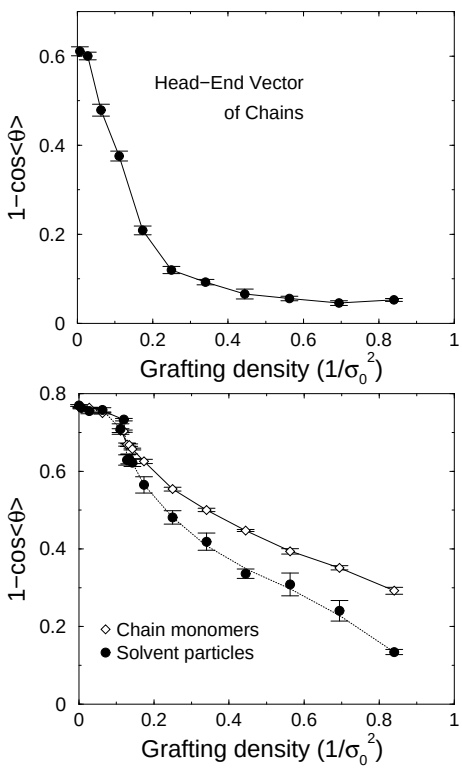

Fig. 6. Average tilt angle $\langle\theta\rangle$ as a function of the grafting density Σ. Top: Head-to-tail vector of grafted chains; Bottom: Single particles.

Acknowledgments

We thank M. P. Allen for invaluable discussions. Furthermore, we have benefitted from useful conversations with K. Binder, D. Johannsmann, J. Rühe, and A. Halperin. M. P. Allen and K. Binder were so kind to let us perform a major part of the simulations on the computers of their groups. This work was funded by the German Science Foundation (DFG).

References

[1] P.-G. de Gennes and J. Prost, *The Physics of Liquid Crystals* (Oxford University Press, Oxford, 1995).

[2] S. Chandrasekhar, *Liquid Crystals* (Cambridge University Press, Cambridge, 1992).

[3] B. Jerome, Rep. Progr. Phys. **54**, 391 (1991).

[4] B. Bahadur (edt.) *Liquid crystals and uses*, World Scientific, Singapore (1990).

[5] M. Schadt, Ann. Rev. Mater. Science, **27**, 305 (1997).

[6] A. Halperin, D. R. M. Williams, Europhys. Lett. **21**, 575 (1993).

[7] A. Halperin, D. R. M. Williams, J. Physics: Cond. Matt. **6**, A297 (1994).

[8] A. Halperin, D. R. M. Williams, Ann. Rev. of Mat. Science **26**, 279 (1996).

[9] B. Peng, D. Johannsmann, J. Rühe, Macromolecules **32**, 6759 (1999).

[10] B. Peng, J. Rühe, D. Johannsmann, Adv. Mater. **12**, 821 (2000).

[11] M. N. Rosenbluth and A. W. Rosenbluth, J. Chem. Phys. **23**, 356 (1955).

[12] D. Frenkel and B. Smit, *Understanding Molecular Simulation*, Academic Press, San Diego, (1996).

[13] H. Lange, Dissertation Universität Mainz, 2001.

[14] C. M. Wijmans, B. Smit, R. D. Groot, J. Chem. Phys. **114**, 7644 (2001).

[15] B. J. Berne and P. Pechukas, J. Chem. Phys. **56**, 4213 (1975).

[16] D. Frenkel, G. C. A. M. Mooij, and B. Smit, J. Phys.: Cond. Matter **4**, 3053 (1992).

[17] H. Lange and F. Schmid, J. Chem. Phys., in print (2002).

[18] H. Lange and F. Schmid, Eur. Phys. J. E **7**, 175 (2002).